The Cryosphere Discussions

The Cryosphere Discussions is the access reviewed discussion forum of *The Cryosphere*

Improving estimation of glacier volume change

M. J. Beedle et al.

Improving estimation of glacier volume change: a GLIMS case study of Bering Glacier System, Alaska

M. J. Beedle[1,4]**, M. Dyurgerov**[2]**, W. Tangborn**[3]**, S. J. S. Khalsa**[1]**, C. Helm**[1]**,
B. Raup**[1]**, R. Armstrong**[1]**, and R. G. Barry**[1]

[1]National Snow and Ice Data Center, 449 UCB, University of Colorado – Boulder, CO
80309-0559, USA
[2]Institute of Arctic and Alpine Research, University of Colorado – Boulder, CO 80309-0450,
USA
[3]HyMet Inc., 13629 Burma Rd. SW, Vashon Island, WA 98070, USA
[4]Geography Program, University of Northern British Columbia, 3333 University Way, Prince
George, B.C. V2N 4Z9, USA

Correspondence to: M. J. Beedle (beedlem@unbc.ca)

Title Page

Abstract	Introduction
Conclusions	References
Tables	Figures

Back | Close

Full Screen / Esc

Printer-friendly Version

Interactive Discussion

EGU

Abstract

The Global Land Ice Measurements from Space (GLIMS) project has developed tools and methods that can be employed by analysts to create accurate glacier outlines and resultant measures of glacier extent. To illustrate the importance of accurate glacier outlines and the effectiveness of GLIMS standards we have conducted a case study on Bering Glacier System (BGS), Alaska. BGS is a complex glacier system aggregated from multiple drainage basins, numerous individual ice streams, and many accumulation areas. Published measurements of BGS surface area vary from 1740 to 6200 km^2, depending on how the boundaries of this system have been defined. Utilizing GLIMS tools and standards we have completed a new outline and analysis of the area-altitude distribution (hypsometry) of BGS using Landsat images from 2000 and 2001. We compared this new outline (3632 km^2) with three previous outlines to illustrate the errors that result from the widely varying estimates used in previous analysis of BGS area. The use of different BGS outlines results in highly variable measures of volume change and net balance (b_n). Outline variability alone results in a net balance rate range of −1.0 to −3.2 m/yr water equivalent (W.E.), a volume change range of −4.2 to −8.2 km^3/yr, and a near doubling in contributions to sea level equivalent (SLE), 0.0122 mm/yr to 0.0236 mm/yr. A study of three different models of BGS net balance leads us to favor estimates of b_n of −1.2 m/yr W.E. and total volume change of −4.2 km^3/yr for the period 1950–2004. These estimates result in a near doubling of contributions to sea level equivalent when compared with previous studies. While current inaccuracies in glacier outlines hinder our ability to fully understand glacier change, there is no reason why our understanding of glacier extents should not be comprehensive and accurate. Such accuracy is possible with the increasing volume of satellite imagery of glacierized regions, and recent advances in tools and standards.

Improving estimation of glacier volume change

M. J. Beedle et al.

EGU

1 Introduction

Glaciers are valuable integrators of their local climate and thus, through their changes, indicators of climate change. Annual field measurements of glacier mass balance have been undertaken in order to monitor annual change, and to understand glacier-climate relationships. Such measurements of glacier mass balance are time consuming, expensive, and arduous. Thus, the vast majority of mass balance programs intentionally select small, easily accessible, well-defined glaciers with little debris-cover (Fountain et al., 1999). This legacy of studying a small subset of "simple" glaciers has resulted in questionable representation of the Earth's complex mountain glaciers. Indeed, few glaciers conform to the simplistic geographies (morphology and hypsometry) of those with detailed mass balance studies.

Complications involved with glacier field measurements, an effort to understand regional trends, and new technology have resulted in many recent studies utilizing remote sensing to study a broader spatial range of glaciers (e.g. Arendt et al., 2002 and Larsen et al., 2007). Such studies have compared two or more glacier surfaces, typically separated on decadal time scales, resulting in vertical height change, volume loss or gain, and an average net balance rate (b_n) for periods between imaging. The glacier surfaces being differenced must be laterally constrained, or in other words, the areal extent of the glaciers must be outlined. Accurate glacier outlining is perhaps the most basic of glacier measurements, but one of significant importance. A glacier's outline yields measurements of surface area and length; and when combined with a digital elevation model (DEM) an outline leads to a glacier's elevation extent and area versus elevation distribution (hypsometry). Perhaps most importantly, a glacier's outline defines the surface area with which any measure of surface height change or mass balance will be integrated to obtain an estimate of a glacier's net balance. Errant glacier outlines result in inaccurate measures of glacier volume change and net balance (Arendt et al., 2006 and Raup et al., 2006). Unfortunately, the seemingly simple task of accurately outlining a glacier meets with many complications.

Complications which hinder an accurate outline include different definitions of what should be included as glacier within an outline and the exceeding complexity of many glacier systems. In this paper we address these two complications by 1) illustrating the facility of a common glacier definition developed by and utilized for the Global Land Ice Measurements from Space (GLIMS) project, and 2) applying this glacier definition to a study of net balance of the complex Bering Glacier System (BGS), Alaska (Fig. 1 and Fig. 2).

1.1 Bering Glacier System

Previous studies have noted the complexity of BGS. In their preliminary inventory of Alaska glaciers, Post and Meier (1980) use BGS as "a particularly extreme example."

"It is in and between two countries (USA, Canada), two major drainages (Pacific, Chitina-Copper), and two major mountain ranges, (Chugach and St. Elias Mountains). Furthermore, the main glacier drainage system has at least five differently named component areas (Steller, Bering, Columbus, Quintino Sella Glaciers, and Bagley Ice Field), and estimates of its total area range from 1740 to 6200 km² depending on how the "Bering Glacier" is defined."

Molnia and Post (1995) present a history of the exploration and study of BGS, a history including early explorers naming portions of the same glacier individually, as a view of the entire glacier was not possible at the time. This history has lead to "the nomenclature associated with the [BGS being] confusing." Some history clarifies how this has come about, and is a sobering reminder of the relative infancy of our ability to view larger glaciers in their entirety.

During the late 19th and early 20th centuries a number of expeditions to the region described and mapped portions of BGS. In 1880 the U.S. Coast and Geodetic Survey named the Bering Glacier in honor of Captain Vitus Bering, an 18th century Danish sea captain. However, the vast expanse of the upper reaches of BGS was not realized until many years later. In the intervening years, expeditions in the region named portions of BGS. For example an expedition in 1897 lead by the Duke of the Abruzzi on

Mt. St. Elias, named a portion of BGS after Christopher Columbus, and a considerable tributary to the Columbus Glacier as the Quintino Sella Glacier after a renowned Italian alpinist (Fig. 2). It was not until 1938, when Bradford Washburn made the first aerial photographs of BGS that a complete view was obtained of the large upper elevation
5 glacier complex that feeds the sprawling piedmont lobe (Molnia and Post, 1995).

Official (U.S. Board on Geographic Names) BGS nomenclature was championed by Austin Post in a significant effort to accurately preserve the history, and honor vital crew-members of Vitus Bering's voyage. Table 1 presents the complete, official Bering Glacier nomenclature. Bering Glacier officially refers to only the piedmont lobe fed by
10 both the Steller Glaciers and main trunk glacier (Central Valley Reach) flowing down from the Bagley Ice Valley (Fig. 3). Previous outlines have incorporated different portions of the BGS. While none of the outlines in this study incorporate the entirety of the official BGS, we refer to them as differently defined outlines of the same glacier (BGS). For this study we outlined a subset of the larger BGS that contributes to what
15 we define as a common terminus (Bering Lobe) for the purpose of mass balance measurements. This outlined area can also be thought of as, and used for studies of, the "surging portion of the Bering Glacier System" or SBG (Fig. 2 and Fig. 7).

Recently, remote sensing, via aerial photography and satellite imagery, has afforded analysts the means of visualizing, outlining and quantifying the entirety of BGS. Unfor-
20 tunately confusion still lingers. Reported surface areas of BGS range from 1740 km^2 upwards to 6200 km^2, with various measurements in between (Post and Meier, 1980; Molnia and Post, 1995; and Arendt et al., 2002).

The official (U.S. Board on Geographic Names) and oft-published surface area of 5173 km^2 makes BGS the largest glacier in Alaska. To put this behemoth in perspective
25 BGS (by this measure) is nearly as large as all the glaciers in Scandinavia and the Alps combined (5286.7 km^2) (Dyurgerov and Meier, 2005).

Recent work (Arendt et al., 2002) has concluded that shrinking Alaska glaciers comprise the largest glacier contribution to global sea level rise yet measured. A few massive coastal glaciers (including BGS) are the biggest culprits. Accurate quantification of

contributions to sea level rise begins with accurate measurements of surface area – by which surface height change and mass balance measurements are integrated. Unfortunately an accurate, consensus measure of BGS surface area has not been realized in recent publications.

1.2 This study

The GLIMS project at the National Snow and Ice Data Center (NSIDC), University of Colorado (Raup et al., 2006; Raup and Khalsa, 2006) is creating standardized methodology and tools, and a common glacier database through which the scientific community can pursue more accurate and more accessible knowledge of glacier parameters and change, leading to better monitoring of the world's glaciers in regards to past, present, and future climatic change. This study, within the broader GLIMS project, aims to address the importance of accurate glacier outlining and hypsometry creation – especially in regards to large, complex glaciers – as well as to demonstrate the facility of GLIMS methodology and tools. To do so we compare the results achieved when integrating net balance estimates (from three different models) with four different BGS outlines and their resultant hypsometries. In addition we examine some of the complicating characteristics of glaciers that do not conform to the simplistic parameters mentioned above, such as debris-cover, surge dynamics, and multiple flow divides.

The comparisons within this study yield: (i) an illustration of the importance of accurate glacier outlining via a common, or at least explicitly stated, glacier definition; (ii) an accurate, transparently-defined outline and hypsometry of the SBG; (iii) SBG volume change results for the second half of the 20th century from three models of mass balance; and (iv) a discussion of, and suggestions on how to mitigate, some of the problems facing the glaciological community in regards to accurately outlining and understanding some of the world's major glaciers.

2 Data

This study uses three previous outlines and resultant hypsometries of BGS, one new BGS outline and resultant hypsometry, and three methods of modeling mass balance to illustrate the potential errors resulting from an inaccurate glacier outline.

2.1 Hypsometries

The following four hypsometries, resulting from individual outlines, are herein named after the first author of the paper in which they first appeared.

The "Arendt" hypsometry (AH) yields a total surface area of 2319 km^2, uses 30.5 m elevation bins beginning at sea level, and has an elevation range of 0 to 1730 m. It should be noted that this outline knowingly encompasses "considerably less than the total area of the [BGS's] hydrological basin" as the outline includes only ice deemed to be well represented by the laster altimetry profiles (Arendt et al., 2002, supporting online text; and Arendt, 2007, personal communication). The AH is included here as a representative of the lower end of the range of previous estimates of BGS surface area. This hypsometry was kindly provided by Anthony Arendt.

The "Tangborn 1" (Tangborn, 2002[1]) and "Tangborn 2" (Tangborn, 1999[2]) hypsometries (T1H and T2H) yield surface areas of 3057 km^2 and 4773 km^2, use 30 m and 50 m elevation bins respectively, and begin at sea level. T1H extends from 0 to 2565 m and T2H extends from 0 to 4650 m. These hypsometries were used in the two studies cited above, but unfortunately it is not known who produced these outlines, or whether digital files of the original outlines exist.

---

[1]A preliminary report. Tangborn, W. V.: Connecting winter balance and runoff to surges of the Bering Glacier, Alaska, Alaska, A preliminary report, HyMet Inc., Seattle, W.A., http://www.hymet.com, 2002.

[2]A preliminary report. Tangborn, W. V.: Mass balance, runoff and internal water storage of the Bering Glacier, Alaska (1950–1996), A preliminary report, Hymet Inc., Seattle, W. A., http://www.hymet.com, 1999.

Title Page

Abstract | Introduction

Conclusions | References

Tables | Figures

◄ | ►

◄ | ►

Back | Close

Full Screen / Esc

Printer-friendly Version

Interactive Discussion

EGU

The "Beedle" hypsometry (BH), produced for this study results in a total surface area of 3632 km^2. The BH hypsometry uses 50 m elevation bins beginning at sea level and has an elevation range of 0 to 4300 m.

A SBG debris cover hypsometry (DCH) was also produced for this study. It has a total surface area of 557 km^2. Both 30 and 50 m elevation bins were used to compare with the four hypsometries discussed above. The SBG DCH has an elevation range of 0 to 1250 m.

2.2 Mass balance models

The PTAA (Precipitation Temperature Area-Altitude) model utilizes precipitation and temperature records from distant lower altitude stations plus a glacier's hypsometry to independently model mass balance (Tangborn, 1999). The PTAA model output used in this study is an average (1950–2004) mass balance gradient, derived from Yakutat and Cordova, Alaska (Fig. 1) meteorological records.

The adjusted PTAA model has been adjusted to incorporate an assumed attenuated ablation rate for the debris-covered area of SBG. Debris-free ice is treated as in the PTAA model, while debris-covered ice is assigned an ablation rate that is an assumed percentage of the PTAA modeled balance gradient.

The template method (Khalsa et al., 2004) utilizes the b_n/accumulation-area ratio (AAR) relationship of a nearby benchmark glacier to extrapolate mass balance of other glaciers in a climatically homogeneous region. Common use of a 1500 m equilibrium line altitude (ELA) – derived from the PTAA model – in both modeling approaches affords comparison between the two methods.

EGU

3 Methods

3.1 Outlining and hypsometry creation

Different glacier definitions will be employed dependent upon the intent of a study. The SBG is outlined here (BH outline) with the intent of being used to quantify the
5 'iceshed' contributing to a unique terminus – Bering Lobe. While the Bering Lobe is a portion of the Bering Glacier (piedmont lobe) it surges and responds to climate change independently of the adjacent Steller Lobe (Fig. 3). In order to understand surges and climatic responses of the Bering Lobe an outline of the contributing ice shed (BH outline) must be used. The BH outline includes the Bering Lobe, the SBG
10 portion of the Central Medial Moraine Band, the Central Valley Reach, the Bagley Ice Valley (including Waxell Glacier, Table 1), the Quintino Sella Glacier, and a portion of the Columbus Glacier (Fig. 2 and Fig. 7). The composite parts of the SBG can also be thought of as the larger BGS without the Steller Glacier, Steller Lobe, and a small portion of the Central Medial Moraine Band deemed attributable to flow from Steller
15 Glacier. In essence the SBG simply incorporates all portions of BGS except those attributable to the Steller Glacier.

The SBG outline created for this study was derived from two Landsat ETM+ images (obtained from the Global Land Cover Facility http://glcf.umiacs.umd.edu/). The first image (acquired 31 August 2000)) was used to digitize the accumulation area. The
20 second image (10 September 2001) was used to digitize the ablation area. Neither image alone covers the entirety of the SBG. The outlined extent comprises all ice that contributes to a common terminus (Bering Lobe) with the intention of being used in studies of glacier mass balance. The SBG outline (BH outline) also adheres to the GLIMS glacier definition developed to reduce inconsistencies in glacier treatment:

25 *"A glacier or perennial snowmass, identified by a single GLIMS glacier ID, consists of a body of ice and snow that is observed at the end of the melt season, or, in the case of tropical glaciers, after transient snow melts. This includes, at a minimum, all tributaries and connected feeders that contribute ice to the main glacier, plus all debris-*

EGU

covered ice. Excluded is all exposed ground, including nunataks. An ice shelf shall be considered as a separate glacier. (Raup and Khalsa, 2006; p. 4)"

More specifically, the glacier definition elaborated on in the GLIMS Analysis Tutorial and employed here, includes 1) ice bodies above bergschrunds that contribute ice and snow to the glacier, 2) connected stagnant ice masses even when supporting an old-growth forest, and 3) all debris covered ice. Excluded are 1) all nunataks, 2) steep rock walls that avalanche snow onto the glacier, 3) all continuous, adjacent ice masses which contribute to a terminus other than the Bering Lobe (i.e. the Steller, Tana, and Malaspina Glaciers), 4) detached, hanging ice masses that may contribute ice via avalanching, and 5) adjacent snowfields, which do not contribute to the mass of BGS. While these standards are suggested by GLIMS and utilized in this study the ultimate glacier definition is to be determined by the analyst, based on objectives and nature of the study. The definition employed here is used in order to discern an individual glacier within a complex glacier system. The reader is directed to the complete GLIMS discussion of glacier definition and analysis standards within the GLIMS Analysis Tutorial[3].

An outline of BGS necessitates a decision as to the inclusion or exclusion of certain levels of glacier karst (Fig. 4), although no standard has been proposed by GLIMS. Stagnant, debris-covered ice bodies, still in contact with the parent glacier, slowly disintegrate via progression of glacier karst; first, growth of debris continues, second, moulins and crevasses develop into sinkholes and then into large water-filled depressions, third, only remnant ice cores remain (Benn and Evans, 1998). In the case of BGS glacier karst progression reaches a mature stage when melt pools erode into one another forming distinctive terminal lakes (e.g. Vitus Lake), definitively delimiting the receding glacier's terminus. At what stage of glacier karst should an adjacent ice body no longer be included as part of the parent glacier? Outlining the entire area of debris-covered, stagnant ice (all levels of glacier karst included) results in an unchang-

---

[3] http://www.glims.org/MapsAndDocs/assets/GLIMS_Analysis_Tutorial_a4.pdf, Raup and Khalsa, 2006.

ing terminus position, until the main body of the glacier pulls away from the stagnant ice mass, then a large "jump" in glacier recession will be noted. For the SBG outline it was decided to draw the outline at the mature stage of glacier karst. Doing so is subjective to the analyst's perception of the continuum of conditions that is mature glacier karst, but serves to provide a progression of terminal disintegration until a definitive terminus can be outlined.

Outlining was done manually using GLIMSView, "A cross-platform application intended to aid and standardize the process of glacier digitization for the GLIMS project" (Raup et al., 2007). GLIMSView is freely available on the GLIMS website (http://glims.org/software/). Previous work (e.g. Paul, 2000; and Albert, 2002) has been done on the accuracy of automated techniques, utilizing manual outlines as a known, accurate benchmark. We used manual outlining to achieve the most-accurate outline possible considering the complexity of BGS, which includes significant debris-cover, forest cover and numerous, complex flow divides. Other studies (e.g. Williams et al., 1991; Williams et al., 1997; and Hall et al., 2003) have investigated errors inherent in outlining glaciers due to complications such as differing ice facies and image resolution, with a focus on accurately delimiting glacier termini from space. In this study we focus more on errors that stem from glacier definition of large, complex glacier systems (such as BGS) as glacier definition is found to play an extremely important role, with potential errors of hundreds to thousands km^2.

USGS topographic maps were used to visually determine the SBG "iceshed", particularly to define flow boundaries between SBG and the adjacent Stellar, Tana, Baldwin, and Malaspina Glaciers. Further refinement and validation of the outline was done by visual analysis of linear surface features indicative of SBG flow, which are apparent on a Landsat ETM+ color composite of bands 4, 3, and 2. This task was aided by band stretching within the histogram function of GLIMSView, particularly in the largely featureless accumulation areas (Fig. 5).

Combination of this outlined area with a composite DEM resulted in the BH. The DEM was created from four stereo Advanced Spaceborne Thermal Emission and Reflection

Radiometer (ASTER) images covering the majority of BGS. Each stereo image was used to generate a corresponding DEM. Gaps were filled with elevation data from the National Elevation Dataset from the USGS.

3.2 Debris-cover hypsometry (DCH)

The DCH was completed from the same 2001 ETM + image, composite DEM, and using the same methodology as that of the BH discussed above. All areas of SBG with continuous (uninterrupted by any visible ice) debris or vegetation cover were outlined and are referred to herein as "debris-cover" (Fig. 4). This definition of debris-cover was chosen for the purpose of delimiting the area of SBG that might be significantly impacted by a reduction of ablation due to a sufficiently thick debris-cover. The DCH was created with both 50 m and 30 m elevation bins in order to compare with the variable elevation bins of the four BGS hypsometries.

3.3 Debris-cover mass balance

It is assumed here that the DCH is composed of a debris mantle that is sufficiently thick (>5–10 cm) to insulate the underlying ice and significantly reduce ablation. Ablation rates of debris covered ice drop dramatically with an increase in debris cover thickness greater than 1 cm to 2 cm (Nakawo and Rana, 1999; Benn and Evans, 1998). In this study the adjustment for debris covered ice ablation is assigned to be one-quarter of the PTAA (see below) modeled mass balance, thus significantly reducing ablation for the debris-covered area (Fig. 4). The intent is to investigate the possible significance of outlining and accounting for debris-cover in remote sensing studies of BGS (and other debris-covered glacier's) mass balance.

EGU

3.4 Mass balance and volume change

3.4.1 PTAA mass balance and volume change

The PTAA model utilizes precipitation and temperature records from distant lower al-
titude stations plus a glacier's hypsometry to model mass balance. The reader is di-
rected to Tangborn (1999) for a complete discussion of the model and applications on
other glaciers. The PTAA model output used in this study is an average (1950–2004)
mass balance gradient, derived from Yakutat and Cordova, Alaska (Fig. 1) meteorolog-
ical records. Field measurements by Fleisher et al. (2005) found an average ablation
rate (1998–2005) near the terminus of SBG (below 100 m) of approximately -10m/yr
which corresponds well with the PTAA modeled (1950–2004 avg.) ablation rate of
between -10.8 m/yr at sea level and -10.0 m/yr at 100 m. In situ measurements of
accumulation are not available to validate the PTAA modeled mass balance gradient
in the accumulation zone. PTAA modeled mass balance results are intrinsically linked
to a glaciers outline, which determines hypsometry. The PTAA model yields realistic
results as the hypsometry exerts a physically real, robust control over mass balance
(Tangborn, 1999).

3.4.2 Debris-cover adjusted PTAA mass balance and volume change

In order to investigate the possible impact of debris-cover on BGS mass balance and
volume change, the PTAA balance gradient is adjusted to reflect attenuated melting
of debris-covered ice (discussed above) resulting in a much flatter balance gradient
for the DCH (Fig. 8). This is done by integrating the debris-cover hypsometry with
the adjusted PTAA balance gradient. Then this DCH total is added to the integration
of the original PTAA balance gradient and the hypsometry of debris-free ice, yielding
a total BGS, DCH adjusted volume change and b_n. This model is incorporated here
to illustrate the importance of accurately outlining significantly debris-covered portions
of glaciers and accounting for such areas in estimates of mass balance and volume

Title Page

Abstract | Introduction

Conclusions | References

Tables | Figures

◄◄ | ►►

◄ | ►

Back | Close

Full Screen / Esc

Printer-friendly Version

Interactive Discussion

EGU

change.

3.4.3 Template method mass balance and volume change

A third method of modeling mass balance, the template method, is used here to further investigate possible measures of BGS volume change, and to illustrate the importance of glacier shape on estimates of mass balance and volume change. The template method relies upon the relationship between b_n and AAR (e.g. Dyurgerov, 1996). A nearby 'benchmark' glacier with annual, in situ, surface mass balance measurements is selected as representative of other glaciers in a climatically homogenous region. The b_n/AAR relationship from the benchmark glacier is applied to the hypsometry of the glacier in question. Of particular importance is the proximity of the benchmark glacier and the assumption that this nearby glacier realistically represents the region's climate. Complete discussions of the template method can be found in Khalsa et al. (2004) and Dyurgerov (1996). Taku, Lemon Creek, Gulkana and Wolverine Glaciers (Fig. 1) (the only glaciers in southern and southeast Alaska with temporally significant mass balance records) were tested as possible benchmarks for BGS. Using either Wolverine or Gulkana Glacier (both with similar distances from and closer to BGS) as the benchmark for BGS yields nearly identical results. The Gulkana Glacier is used here because the in situ measurements agree best (qualitatively) with laser altimetry studies (Arendt et al., 2002) as well as being best correlated with modeled BGS b_n(r=0.62)[4]. Correlation coefficients between modeled BGS b_n and the other in situ records are 0.45 (Lemon Creek Glacier), 0.38 (Taku Glacier), and 0.37 (Wolverine Glacier).

3.5 Percent of Alaska contribution to sea level equivalent

The percent of Alaska glacier contribution to sea level equivalent (SLE) attributable to BGS was calculated based on a total Alaska contribution of 0.14 mm/yr, which Arendt

---

[4]This modeled BGS b_n was derived via the PTAA model (Tangborn, 1999), but annually for the period 1950 to 2000, as opposed to the 1950–2004 average b_n used in this study.

EGU

et al. (2002) found for the period from the mid-1950s to the mid-1990s. The same study found a nearly doubled rate (0.27 mm/yr) of SLE contributions from the mid-1990s to 2000–2001. The former rate (0.14 mm/yr) was used here as the time period (mid-1950s to the mid-1990s) better matches that of the average 1950 - 2004 PTAA modeled mass balance gradient.

4 Results

4.1 Geographical statistics of Bering Glacier System outlines and hypsometries

BGS, as defined and outlined here (BH outline) from 2000 and 2001 imagery, is 3632 km^2 – much less (30%) than the official 5173 km^2 that is frequently published. This outline and the resultant BH have an elevation range of 0–4300 m (Table 2). Nunataks outlined and excluded from the BH outline total 123 km^2 or 3% of the total surface area. The debris-cover outline has an elevation range of 0 to 1150 m and an area of 557 km^2, 15% of the total BGS area.

Possible variability in outlining the complex BGS was estimated to not exceed ±330 km^2, or 9% of the BH surface area. This error estimate accounts for different possible outlines within glacier karst and debris/vegetation cover of the piedmont lobe, errant divide assessment, divide migration during surges, and inclusion or exclusion of nunataks. Additional details on these estimates are given later.

Unfortunately, published values of BGS surface area vary by more than a factor of three. And the subset of four outlines used in this study (Table 2) vary by a factor of two (2319 km^2 to 4772 km^2). Such variability strays significantly from our estimated error of ±330 km^2.

While the four outlines begin at sea level their uppermost elevations vary from 1737 m to 4650 m. Dividing the accumulation and ablation areas by an ELA at 1500 m results in relatively similar ablation areas (2048–2561 km^2) and highly variable accumulation areas (271–2211 km^2).

Improving estimation of glacier volume change

M. J. Beedle et al.

Title Page

Abstract	Introduction
Conclusions	References
Tables	Figures

◄◄   ►►

◄   ►

Back   Close

Full Screen / Esc

Printer-friendly Version

Interactive Discussion

EGU

Steady state AARs generally are between 50 and 80 (percent accumulation area), with typical values between 55 and 65, and glaciers with debris-covered termini generally have lower AARs (<40) (Benn and Evans, 1998). The AARs of 12 and 22 for the AH and T1H outlines are extremely low, while AARs of 43 and 46 for the BH and T2H outlines are more reasonable, especially when considering the significant area (15% of total) of debris-cover on the lower reaches of BGS.

4.2   Net balance and volume change

Highly variable measures of b_n and volume change result from the use of different BGS outlines and resultant hypsometries (Tables 3–5). Integration of the four hypsometries with modeled mass balance results in a b_n range of –1.0 to –4.4 m/yr water equivalence (W.E.), and volume change of –4.2 to –11.2 km^3/yr. Each integration between one of the three mass balance models (PTAA, debris-cover adjusted, and template method) and the four hypsometries reveals the same pattern of results: 1) the AH always has the most negative b_n, while 2) the T2H always has the least negative b_n, and 3) the T1H always has the greatest volume change, while 4) the BH always has the least volume change.

Use of the PTAA modeled mass balance gradient with the four hypsometries results in the greatest BGS net mass loss. PTAA b_n rates range from –1.6 to –4.4 m/yr W.E. and volume change rates range from –7.3 to –11.2 km^3/yr (Table 3).

Adjusting the PTAA modeled mass balance gradient for debris-cover results in a significant decrease in net mass loss, with the ranges of b_n results changing to –1.0 to –3.2 m/yr W.E. and volume change to –4.2 to –8.2 km^3/yr (Table 4).

Use of the template method results in estimates of BGS b_n and volume change similar to that of the debris-cover adjusted PTAA model. b_n ranges from –1.1 to –3.0 m/yr W.E. and volume change rates range from –4.4 to –7.6 km^3/yr (Table 5).

EGU

5 Discussion

5.1 Geographical statistics

BGS geographical statistics from the BH are significantly different from those published previously. Here we discuss potential errors in the BH, why disparities exist between measures of BGS surface area, and implications of these results.

5.1.1 Potential errors of the BH outline

How accurate is the outline produced for this study and the resultant BH? A perfectly accurate outline of a glacier is unobtainable, except perhaps in the case of a small, terrestrially constrained glacier with no snow cover to obscure the glacier boundary. We feel the outline prepared for this study (of SBG) and the resultant BH is as accurate as possible with the basic tools and products necessary for analysis of glacier extent – GLIMSView (manual outlining), satellite imagery, and a DEM.

The complex divide between BGS and Tana Glacier (Fig. 6) heavily biases our error margin of $\pm 330\,\mathrm{km}^2$ (9% total glacier area). Different outlines of this single flow divide may vary by as much as $\pm 200\,\mathrm{km}^2$. Previous outlines of BGS may have included the entirety of the Bagley Ice Valley, unrealistically diminishing the Tana Glacier's accumulation area. The estimated error of $\pm 330\,\mathrm{km}^2$ includes this unrealistic outline, and therefore may be overly conservative.

The greatest likelihood of errors in the BH outline stems from measurement difficulties of the accumulation area. Snow cover at upper elevations hinders accurate detection of glacier outlines. Adjacent snowfields, which do not contribute to BGS, may erroneously be included. Such errors serve to increase the accumulation area, resulting in higher AAR values, and more positive mass balance measurements.

Another likely source of error exists when outlining near ridge crests on steep, shaded slopes. The BH outline may include areas of steep snow covered rock slopes that contribute to BGS via avalanching, or negate areas of BGS masked by shadow.

Improving estimation of glacier volume change

M. J. Beedle et al.

Title Page

Abstract	Introduction
Conclusions	References
Tables	Figures

◄◄   ►►

◄   ►

Back   Close

Full Screen / Esc

Printer-friendly Version

Interactive Discussion

EGU

These areas are extremely small relative to total glacier area, and assumed here to be negligible.

A final source of possible error in the BH outline is not extending to appropriate upper elevations, as revealed by the extent of the T2H outline, which reaches 350 m higher. Elevations of 4,650 m (T2H outline) within BGS ice-shed can only be reached in the immediate vicinity of the summit of King Peak (5173 m) (Fig. 2), thus any error in the BH outline at these elevations would have very little impact on BGS surface area.

5.1.2 Disparities between four BGS outlines

Why do BGS areas differ by a factor of three? Primarily this is caused by disparate glacier definitions. Secondary causes of such disparities include errors that stem from the use of different products, tools, and methods employed for outlining, and actual changes in glacier extent.

Even when a common definition is not used to create glacier outlines, transparent understanding of the glacier's extent can be realized through the explicit statement of the employed definition. Molnia and Post (1995) provide such a definition for the BGS outline that results in the official published surface area of 5173 km^2.

"We define the Bering Glacier system based on drainage-basin analysis, divide topography, ice-surface moraine patterns, and ice elevation and flow lines. We include: all of the Steller Glacier, virtually all of the Bagley Icefield (including the Quintino Sella Glacier, but excluding a small northward-flowing section of the icefield that feeds the Tana Glacier and an unnamed distributary draining north to Logan Glacier), and the area described by the [U.S.] Board [on Geographic Names] as the 'Bering Glacier' in 1932." (Molnia and Post, 1995; p. 98)"

Via this definition of BGS we know that this outline includes Steller Glacier (Fig. 2), which is estimated to be 824 km^2, and is deemed a separate glacier within the glacier definition employed here. It is uncertain whether this outline includes or excludes nunataks. Nunataks total 123 km^2 in the BH outline. Subtracting these two areas from the Molnia and Post (1995) total (5173 km^2) results in a Bering Glacier area of

4227 km^2. When taking into account the margin of error in accurately outlining the Tana/BGS divide (discussed above), the 5173 km^2 outline might dwindle to nearly the upper bound of the BH outline margin of error (3962 km^2). And, indeed, Molnia and Post (1995) state that the tributaries of the 350 km^2 Bering Glacier piedmont lobe total

5 3620 km^2, equaling a total area of 3970 km^2. Thus, glacier definition explains the majority of the variance between the BH outline (3632 km^2) and the official area (5173 km^2).

Another, separate BGS definition, is that of Arendt et al. (2002), which results in a surface area of 2319 km^2, and is included in this study (AH). This glacier definition is discussed in the online supporting text in regards to both BGS and Malaspina Glacier:

10 *"Our outlined areas for these two glaciers are considerably less than the total area of their glacierized hydrological basins, because we terminated the outlines at the uppermost elevation contours that our profiling sampled. (Arendt et al., 2002; online supporting text p. 6)"*

Such an outline results in very little accumulation area, an unrealistic AAR, and

15 increased negative mass balance. It should be mentioned here that the Arendt et al. study was of regional mass balance and that "the uppermost areas of these glaciers are accounted for in the St. Elias regional extrapolation, based on data from nearby glaciers (Arendt et al., 2002; online supporting text p. 6)."

Glacier outlines may differ significantly depending upon inclusion or exclusion of ice

20 free nunataks within the outlined glacier boundary. While excluded nunataks within the BH outline total only 123 km^2 (3% of the total area) other glaciers may have much larger nunatak areas and exclusion or inclusion of these areas has the potential for significant errors.

Unfortunately we could find neither an outline, nor glacier definition of either the T1H

25 or T2H outlines. Without direct comparison of the four outlines – such as a composite image containing each outline – it is difficult to conclusively discern where and how the outlines differ. However, it is apparent from the discrepancies in elevation range and accumulation area (Table 2) that the four outlines in this study differ primarily at upper elevations. The AH and T1H outlines do not include the upper elevation accumulation

EGU

area, whereas the BH and T2H outlines extend to similar upper elevations.

In addition to different glacier definitions, analysis errors also stem from the use of different tools and products. Digitization of glacier outlines can either be done manually or via an array of automated techniques (e.g. Albert, 2002). Manual digitization is still the most accurate tool for extracting accurate glacier outlines, but is also tedious and time consuming (Raup et al., 2007). While automated techniques are rapid and consistent, they can falter with regards to ambiguous surfaces, particularly the delineation of debris-covered ice (e.g. Whalley and Martin, 1986; and Sidjak and Wheate, 1999).

BGS terminus retreat and advance may be a primary reason for disparities between the ablation areas of the four outlines used in this study. BGS surge dynamics, which have resulted in dramatic terminus advance followed by rapid retreat have driven surface area changes of greater than $100 \, km^2$ (Molnia and Post, 1995). Such dramatic changes in surface area, which occurred at least six times during the 20th century, may explain a significant portion of the increased ablation areas of the T1H and T2H outlines, which were likely created from older images.

Use of different glacier definitions is the single largest factor resulting in disparate measures of glacier surface area, differences that can lead to significant errors in estimation of glacier mass balance.

5.1.3 Largest glacier in the United States?

BGS (frequently referred to as Bering Glacier) is often listed as the largest glacier in the United States at $5173 \, km^2$, with the neighboring Malaspina Glacier number two at $5000 \, km^2$ (Molnia, 2001). Our BGS area of $3632 \, km^2$ (SBG) may seem to alter this statistic, but measures of Malaspina Glacier suffer from the same complications of glacier definition as those discussed above for the Bering Glacier. The greater Malaspina Glacier system has also been historically composed of numerous, separately named glaciers, including the Columbus, Seward, Agassiz, and Malaspina Glaciers, all of which comprise the larger glacier system, similar to the confusing nomenclature of BGS. Previous estimates of Malaspina Glacier area typically include

the portion of the massive piedmont lobe attributable to the Agassiz Glacier. Using the same methodology as employed to outline the BGS results in a Malaspina Glacier area of 3220 km^2, significantly less than our BGS surface area.

5.2 Bering Glacier System volume change

Our results show wide-ranging differences in estimates of BGS volume change, depending upon variability among outlines and mass balance models. Here we firstly discuss variability that is due solely to differently outlined areas and resultant hypsometry, then variability attributable to the different methods of modeling mass balance, and finally, implications of these results.

5.2.1 Variability due to different outline areas and hypsometry

In this section we use template method modeled mass balance results (Table 5) to illustrate this point. We find average b_n results varying from –1.1 to –3.0 m/yr W.E. and average volume change of –4.4 to –7.6 km^3/yr (Table 5), dependent upon BGS outline and resultant hypsometry. This is not surprising, but simply illustrates the importance of accurate glacier outlines, especially with regard to recent efforts to accurately discern contributions of mountain glaciers to SLE.

Regardless of mass balance model, a common pattern is realized between the four outlines and their hypsometries. The AH always has the most negative b_n, while the T2H always has the least negative b_n. The results for b_n are not surprising in that the outline that over samples the ablation area to the utmost (AH) and has the lowest AAR (12) is the most negative (–3.0 m/yr W.E.) and the outline that incorporates the most area above the ELA (T2H) and has the highest AAR (46) is the least negative (–1.1 m/yr W.E.). Interestingly a different pattern is realized with regard to volume change.

The T1H always has the greatest volume change, while the BH always has the least volume change. This difference is due to outlining variability within the ablation area and the importance of high ablation rates near the terminus, rates that are nearly 5

EGU

times that of the highest, counteracting accumulation rates at upper elevations. The T1H outline has the most negative volume change ($-7.6\,km^3$/yr), greater even than that of the AH as the T1H incorporates a great deal more ablation area at very low elevations where ablation rates are greatest (Table 2). The BH outline has the least negative volume change ($-4.4\,km^3$/yr), less negative than that of the T2H outline with significantly more accumulation area, as the T2H outline incorporates a great deal more area within the important ablation area.

Accurate glacier outlines are obviously extremely important to our understanding of the volume change and mass balance of any glacier. Indeed, BGS outline variability plays a greater role in determining mass balance estimates than the mass balance models utilized in this study.

5.2.2 Variability due to different mass balance models

The three mass balance models used in this study provide different results, all of which are negative, regardless of outline and model. Each of these models has unique assumptions, which highlight the importance of accurate glacier outlines and differently impact results. Here we discuss the variability of these results, the assumptions that lead to these results and make some comparisons with previous studies in order to arrive at a best guess of SBG's mass balance. To do so we utilize the results for only the BH outline, which have a b_n range of -1.2 to -2.0 m/yr W.E.

The PTAA model (unadjusted) results in the most negative b_n (-2.0 m/yr W.E.) and the greatest volume change ($-7.3\,km^3$/yr) (Table 3). Reliance upon distant, sea-level meteorological stations likely biases this model towards more negative mass balance results, especially in such a topographically extreme region where precipitation will be highly variable, and may be significantly greater at upper elevations. Different studies have shown very high annual precipitation in the St. Elias Mountains. Mayo (1989) cites National Weather Service data of 2–6 m mean annual precipitation and the PRISM map (Daly et al., 1994) for Alaska and Yukon Territroy, Canada indicates that BGS accumulation area receives between 5 and 13 m of precipitation annually. Thus, it is possible

Improving estimation of glacier volume change

M. J. Beedle et al.

Title Page

Abstract	Introduction
Conclusions	References
Tables	Figures

|◀ | ▶|

◀ | ▶

Back | Close

Full Screen / Esc

Printer-friendly Version

Interactive Discussion

EGU

that the PTAA model underestimates accumulation above the ELA on BGS. Tangborn (1999) found the PTAA model to consistently reveal a more negative mass balance than the field measured mass balance of South Cascade Glacier, Washington, due to the models "much greater ice ablation on the lower glacier." With field measure-

5 ments (Fleisher et al., 2005) of BGS ablation corroborating PTAA modeled ablation we assume that the more-negative PTAA results likely stem from underestimation of accumulation. Other studies (Tangborn, 1997 and Tangborn and Post, 1998), find PTAA simulated accumulation balance to agree within 0.2 m W.E. for point measurements over a 5-year period on the Columbia Glacier, Alaska. Additional, in situ, observations

10 of precipitation are needed to understand accumulation rates of the upper elevations of BGS and other glaciers, which originate in the topographically significant St. Elias Mountains.

The adjusted (for debris-cover) PTAA model results in less negative b_n (–1.2 m/yr W.E.) and volume change (–4.2 km^3/yr) (Table 4). This is due to the significant attenu-

15 ation of ablation assigned to the 557 km^2 of debris-cover, illustrating that the insulating effects of debris-cover can be extremely important in assessments of mass balance of glaciers with significantly debris-covered areas. The debris-cover adjustment assigned here results in a 3.1 km^3/yr reduction in volume loss when compared with the unadjusted PTAA modeled result.

20 Arendt et al. (2002) found thinning rates on the Malaspina Glacier piedmont lobe to be similar on both debris-covered ice and nearby clean ice areas at the same elevation, and therefore included the debris-covered ice of BGS in their volume change estimates without sampling this area (online supporting text, p. 6). This result contradicts our debris-cover ablation rate assumptions, suggesting that debris-cover (at

25 least that which was characterized by the sampled portion of Malaspina Glacier) may not have a significant impact on ablation rates, or that a dynamical process hinders detection of ablation when assessing surface height change.

Using the relative surface elevation of the Central Medial Moraine Band and the adjacent Bering and Steller Lobes, Austin Post (personal communication, 2007) found

Title Page

Abstract | Introduction

Conclusions | References

Tables | Figures

◄◄ | ►►

◄ | ►

Back | Close

Full Screen / Esc

Printer-friendly Version

Interactive Discussion

EGU

the debris covered ice to have an ablation rate roughly half that of the adjacent clean ice. This ablation estimate is double that of our assumed debris-cover ablation rate of one-quarter of clean ice ablation rates.

Kayastha et al. (2000) find a 40-cm-thick debris-cover to reduce ablation rates by one-third, and negligible ablation rates for a debris-cover greater than one meter. This result suggests that our outlined debris-cover area must be in excess of 40 cm thick for our estimated ablation rate of one-quarter that of clean ice to be valid.

While not fully understood, it is revealed here that accurate assessment of debris-cover ablation rates, and accurate outlining of debris-cover, is imperative in studies of volume change on glaciers with significant debris-cover.

Template method estimates of SBG mass balance are also less negative than the PTAA model results with a b_n of −1.2 m/yr W.E. and volume change of −4.4 km^3/yr (Table 5), very similar to those from the debris-cover adjusted PTAA model. Assumptions within the template method that may impact the accuracy of these estimates include benchmark glacier proximity, climatic regime, and glacier shape/hypsometry.

Gulkana Glacier, used here as the benchmark for BGS, is located approximately 350 km north north-west in a continental climatic zone (Fig. 1). The Gulkana Glacier mass balance record correlates best with annual, PTAA modeled SBG mass balance. In addition, template method b_n for the AH (−3.0 m/yr W.E.) compares well with the b_n found by Arendt et al. (2002) for the period 1995–2000 (−2.8 m/yr W.E.)[5]. Regardless of such favorable comparisons, it seems implausible that such a distant, continental glacier would serve well as a benchmark for mass balance of the maritime BGS. Using the maritime Wolverine Glacier as the benchmark, however, yields template method modeled BGS results nearly identical to those which employ the Gulkana Glacier as the benchmark. This may be due to the importance of glacier shape in the template method and the similar pie shape of both the Gulkana and Wolverine Glaciers.

The shape of a glacier, revealed via an accurate outline and quantified by its hyp-

[5]Presented as an ice equivalent in Arendt et al. (2002) of −3.1 m/yr. A conversion to water equivalent results in an approximate b_n of −2.8 m/yr W.E.

EGU

sometry, will impact how glaciers within a common climatic region integrate climatic inputs, and thus will respond differently. Gulkana Glacier is generally pie shaped – with area increasing with elevation, whereas BGS is more rectangular, with similar surface area regardless of elevation. A pie-shaped glacier will preferentially weight the larger upper elevation accumulation areas, whereas a rectangular glacier will equally weight the evenly distributed areas, thus an identical AAR will not necessarily result in common mass balance. For example, within the template method, the SBG AAR of 43 (resulting from a 1500 m ELA and the BH) is assigned to have a b_n resulting from an AAR of 43 on the Gulkana Glacier; however it is unlikely that the b_n/AAR relationship will be identical on glaciers with different shapes. The use of Gulkana Glacier as a benchmark for BGS may have resulted in slightly less negative mass balance results, as the Gulkana Glacier b_n/AAR relationship will reflect the preferential weighting of upper elevation areas due to its shape.

The three models utilized in this study have individual assumptions inherent to each, with different impacts upon accuracy. Due to such assumptions and associated possible errors, we favor the estimates of volume change and mass balance from the similar adjusted PTAA model and template method integrated with the BH. Based upon these two models we find SBG b_n to have averaged −1.2 m/yr W.E. with volume change of −4.2 to −4.4 km^3/yr for the period 1950–2004.

5.2.3 Implications

Previous studies (Arendt et al., 2002 and Larsen et al., 2006) have illustrated the dramatic net mass loss from Alaska glaciers and associated contributions to SLE. Arendt et al. (2002) find BGS volume change to be −1.5 km^3/yr from 1972 to 1995 and −5.97 km^3/yr from 1995 to 2000, resulting in a total net mass loss of −64.8 km^3 for the 28-year period from 1972 to 2000. Larsen et al. (2006) find that glacier thinning in southeast Alaska is about double that of the Arendt et al. (2002) study due primarily to an under-representation of calving glaciers.

Estimates of contributions to SLE (using the adjusted PTAA model) range from

0.0122 mm/yr (BH) to 0.0236 mm/yr (T1H), or total SLE from 0.659 mm and 1.274 mm respectively (Table 4). These SLE contributions range from 8.7% to 16.9% of the total contribution to SLE of all Alaska glaciers. This illustrates how accurate understanding of mountain glacier contributions to SLE is dependent upon accurate glacier outlines.

Favoring the rate of volume change resulting from the adjusted PTAA model integrated with the BH of -4.2 km^3/yr (which is the least negative volume loss within this study) we find a total SBG 1972–2000 volume loss of -117.6 km^3, nearly double the Arendt et al. (2002) results for the same period. While this result is for only one glacier, it is possible that previous measures (Arendt et al., 2002) significantly underestimate contributions to SLE from Alaska glaciers, echoing the conclusions of other studies (Larsen et al., 2006). The disparity between our results and those of Arendt et al. (2002), however, is due to the differences between laser altimetry of glacier surface height change and mass balance models as opposed to complications with regional extrapolation from a limited set of altimetry profiles. It must be noted, that while results here indicate a possible underestimation of contributions to SLE (by .1463 mm from 1972–2000), errant glacier outlining and model differences can just as readily result in overestimation of contributions to SLE.

6   Conclusions

Accurate glacier outlines and hypsometries are imperative in order to understand mass balance, volumetric change, eustatic sea level rise, and relationships between changes in such measures and climate. To illustrate this point, we have used the complex BGS as a case study. Mass balance results for four different BGS outlines show widely differing results in b_n, volume change, and contributions to SLE. Outline variability alone results[6] in a b_n range of -1.0 to -3.2 m/yr W.E., a volume change range of -4.2 to -8.2 km^3/yr, and a near doubling in contributions to SLE, 0.0122 mm/yr to 0.0236 mm/yr.

---

[6]Results from the debris-cover adjusted PTAA model.

EGU

Such variability, in the case of BGS, stems primarily from the use of different glacier definitions.

The surface area of the SBG is found here to be 3632 km^2, significantly less than the official area of BGS (5173 km^2), but mid-range between previous estimates (1720 to 6200 km^2). This new outline and associated hypsometry, when integrated with the favored template method and adjusted PTAA models, result in SBG mass balance of –1.2 m/yr W.E. and an annual volume change of approximately –4.2 km^3/yr for the period 1950–2004. This volume change results in an estimate of SLE that is nearly double that of previous estimates (Arendt et al., 2002).

While BGS is an extreme case study, it is likely that the lack of an accurate outline extends to other large, important glaciers in Alaska and beyond. This point is illustrated here by our preliminary measure of Malaspina Glacier surface area, which we find to be 3262 km^2, significantly less than the frequently published 5000 km^2. Utilization of GLIMS tools and techniques will help in future assessment of glacier extents and change.

The GLIMS project's methods, tools, and database, which were employed for this study, serve to standardize glacier definition, provide a user-friendly digitization tool (GLIMSView), and make glacier outlines (and subsequent geographical statistics) widely available to potential analysts via a common database. Utilization of these GLIMS standards will result in a much-improved understanding of the extent of the world's glaciers, assessment of how and why they are changing, and potential human impacts stemming from such changes (such as eustatic sea level rise).

It is imperative that analysts continue to study mass balance of large complex glaciers and glacier systems, which represents a significant advance when compared with the legacy of detailed studies on small, simple, supposedly representative glaciers. To do so, however, we must begin with accurate glacier outlines. Such outlines – as are being produced through the GLIMS project – will be a valuable platform from which we can gain a much more accurate understanding of glacier extents, changes in extent, drivers of such changes, and implications of these changes.

EGU

With increasing satellite imagery coverage of glacierized regions, advances in tools such as GLIMSView, and employment of GLIMS standards there is no reason why our understanding of glacier extents should not be comprehensive and accurate.

References

Albert, T.: Evaluation of remote sensing techniques for ice-area classification applied to the tropical Quelccaya ice cap, Peru, Polar Geog., 26, 3, 210–226, 2002.

Arendt, A. A., Echelmeyer, K. A., Harrison, W. D., Lingle, C. S., and Valentine, V. B.: Rapid wastage of Alaska glaciers and their contribution to rising sea level, Science, 297, 382–386, 2002.

Arendt, A., Echelmeyer, K., Harrison, W., Lingle, C., Zirnheld, S., Valentine, V., Ritchie, B., and Druckenmiller, M.: Updated estimates of glacier volume changes in the western Chugach Mountains, Alaska, and a comparison of regional extrapolation methods, J. Geophys. Res., 111, F03019, doi:10.1029/2005JF000436, 2006.

Benn, D. I. and Evans, D. J. A.: Glaciers and glaciation, Arnold Publishers, New York, NY. 1998.

Daly, C., Neilson, R. P., and Phillips, D. L.: A statistical-topographic model for mapping climatological precipitation over mountainous terrain, J. Appl. Meteorol., 33(2), 140–158, 1994.

Dyurgerov, M.: Substitution of long-term mass balance data by measurements of one summer, Z. Gletsch., 32, 177–184, 1996.

Dyurgerov, M. B. and Meier, M. F.: Glaciers and the changing earth system: A 2004 snapshot, Institute of Arctic and Alpine Research, University of Colorado, Occasional Paper No. 58, 2005.

Fleisher, P. J., Bailey, P. K., Natel, E. M., Miller, J. R., and Tracy, M. W.: Post-surge field measurements of ablation and retreat, eastern sector, Bering Glacier, Alaska, Abstracts with program, Geological Society of America, 37(7), 423, 2005.

Improving estimation of glacier volume change

M. J. Beedle et al.

Title Page

Abstract | Introduction

Conclusions | References

Tables | Figures

|◄ | ►|

◄ | ►

Back | Close

Full Screen / Esc

Printer-friendly Version

Interactive Discussion

EGU

Fountain, A. G., Jansson, P., Kaser, G., and Dyurgerov, M.: Summary of the workshop on methods of mass balance measurements and modeling, Tarfala, Sweden August 10–12, 1998, Geogr. Ann. A, 81(4), 461–465, 1999.

Hall, D. K., Bayr, K. J., Schöner, W., Bindschadler, R. A., Chien, J. Y. L.: Consideration of
errors inherent in mapping historical glacier positions in Austria from the ground and space (1893–2001), Remote Sens. Environ., 86, 566–577, 2003.

Kayastha, R. B., Takeuchi, Y., Nakawo, M., and Ageta, Y.: Practical prediction of ice melting beneath various thickness of debris cover on Khumbu Glacier, Nepal, using a positive degree-day factor, Debris-covered glaciers, proceedings of a workshop held at Seattel, Washington,
USA, September 2000, IAHS Publ. no. 264, 71–81, 2000.

Khalsa, S. J. S., Dyurgerov, M. B., Khromova, T., Raup, B. H., and Barry, R. G.: Space-based mapping of glacier changes using ASTER and GIS tools. IEEE T. Geosci. Remote, 42(10), 2177–2183, 2004.

Larsen, C. F., Motyka, R. J., Arendt, A. A., Echelmeyer, K. A., and Geissler, P. E.: Glacier
changes in southeast Alaska and northwest British Columbia and contribution to sea level rise. J. Geophys. Res., 112, F01007, doi:10.1029/2006JF000586, 2007.

Molnia, B.: Glaciers of Alaska, Alaska Geogrpahic, 28(2), 144p., 2001.

Molnia, B. F. and Post, A.: Holocene history of Bering Glacier, Alaska: A prelude to the 1993–1994 surge. Phys. Geogr., 16(2), 87–117, 1995.

Muskett, R. R., Lingle, C. S., Tangborn, W. V., and Rabus, B. T.: Multi-decadal elevation changes on Bagley Ice Valley and Malaspina Glacier, Alaska, Geophys. Res. Lett., 30(16), 1857, doi:10.1029/2003GL017707, 2003.

Nakawo, M. and Rana, B.: Estimate of ablation rate of glacier ice under a supraglacial debris layer, Geogr. Ann. A, 81(4), 695–701, 1999.

Østrem, G. and Brugman, M.: Glacier mass-balance measurements: A manual for field and office work, National Hydrology Research Institute, Canada. Science Report No. 4., 1991.

Post, A. and Meier, M. F.: A preliminary inventory of Alaskan Glaciers. Proceedings of the Riederalp Workshop, September 1978, IAHS-AISH Publ. No. 126, 45–47, 1980.

Raup, B. and Khalsa, S. J. S.: GLIMS analysis tutorial, 2006.
http://www.glims.org/MapsAndDocs/assets/GLIMS_analysis_tutorial.pdf.

Raup, B., Rocoviteanu, A., Khalsa, S. J. S., Helm, C., Armstrong, R., and Arnaud, Y.: The GLIMS geospatial glacier database: A new tool for studying glacier change, Global Planet. Change, 56, 101–110, doi:10.1016/j.gloplacha.2006.07.018, 2006.

EGU

Raup, B., Kääb, A., Kargel, J. S., Bishop, M. P., Hamilton, G., Lee, E., Paul, F., Rau, F., Soltesz, D., Khalsa, S. J. S., Beedle, M., and Helm, C.: Remote sensing and GIS technology in the Global Land Ice Measurements from Space (GLIMS) project, Comput. Geosci., 33, 104–125, 2007.

5 Sidjak, R. W. and Wheate, R. D.: Glacier mapping of the Illecillewaet icefield, British Columbia, Canada, using, Landsat TM and digital elevation data, Int. Jour. Remote Sens., 20, 273–284, 1999.

Tangborn, W. V.: Using low-altitude meteorological observations to calculate the mass balance of Alaska's Columbia Glacier and relate it to calving and speed, In: Calving Glaciers: Report

10 of a Workshop, February 28-March 2, 1997, edited by: Van der Veen, C. J., (BPRC Report No. 15, Byrd Polar Research Center, The Ohio State University, Columbus, Ohio), 141–161, 1997.

Tangborn, W. V.: A mass balance model that uses low-altitude meteorological observations and the area-altitude distribution of a glacier, Geogr. Ann. A, 81(4), 753–765, 1999.

15 Tangborn, W. V. and Post, A. P.: Iceberg prediction model to reduce navigation hazards: Columbia Glacier, Alaska. Ice in Surface Waters, Volume 2, Proceedings of the 14th International Symposium on Ice, Potsdam New York, July 17–31, 1998.

Whalley, W. B. and Martin, H. E.: The problem of hidden ice in glacier mapping, Ann. Glaciol., 8, 181–183, 1986.

20 Williams Jr., R. S., Hall, D. K., and Benson, C. S.: Analysis of glacier facies using satellite techniques, J. Glaciol., 37(125), 120–128, 1991.

Williams, R. S. Jr., Hall, D. K., Sigurdsson, O., and Chien, J. Y. L.: Comparison of satellite-derived with ground-based measurements of the fluctuations of the margins of Vatnajökull, Iceland, Ann. Glaciol., 24, 72–80, 1997.

Improving estimation of glacier volume change

M. J. Beedle et al.

Title Page

Abstract | Introduction

Conclusions | References

Tables | Figures

◄◄ | ►►

◄ | ►

Back | Close

Full Screen / Esc

Printer-friendly Version

Interactive Discussion

EGU

Table 1. Official Bering Glacier System nomenclature. This table describes the Official (U.S. Board on Geographic Names) Bering Glacier System nomenclature and definition of the component parts of the Surging Bering Glacier System (SBG).

Official Bering Glacier System Nomenclature

Name	Description
Bering Glacier	Entire piedmont lobe (Bering Piedmont Glacier), including Steller and Bering Glacier Piedmont Lobes
Steller Lobe	Portion of piedmont lobe portion fed by Steller Glacier
Steller Glacier	Tributary feeding Steller Lobe
Central Medial Moraine Band	Moraine covered ice between Steller and Bering Lobes
Bering Lobe	Portion of piedmont lobe fed by the main trunk glacier
Central Valley Reach	Central portion of main trunk glacier feeding Bering Lobe
Bagley Ice Valley	Main accumulation area both east and west
Waxell Glacier	West branch of Bagley Ice Valley
Bering Glacier System	Entire glacier flowing to the Bering Piedmont Glacier
Bagley Ice Field	Entire icefield from the Copper River to approximately the Canadian Border

Portion of Bering Glacier System outline utilized in this study

Surging Bering Glaciery System (SBG)	Surging portion of the Bering Glacier System including Bagley Ice Valley, Central Valley Reach, Bering Lobe, portions of the Central Medial Moriane Band, the Quintino Sella Glacier and portions of the Columbus Glacier

EGU

EGU

Table 2. Geographic statistics of four Bering Glacier System outlines. Total Bering Glacier System surface area varies by up to a factor of two within the subset of outlines used for this study. Elevation range, ablation area, and accumulation area differences indicate the primary disparity between outlines is in the accumulation area. Ablation area, accumulation area, and AAR all assume an ELA of 1500 m.

Outline/ Hypsometry	Total Area (km^2)	Elevation Range (m)	Ablation Area (km^2)	Accumulation Area (km^2)	AAR (ELA 1500 m)
AH	2319	0–1737	2048	271	12
T1H	3057	0–2565	2383	674	22
BH	3632	0–4300	2080	1552	43
T2H	4773	0–4650	2561	2211	46
DCH	557	0-1150	557	0	0

Table 3. PTAA model mass balance results. Mass balance, volumetric change, and SLE results from integrating the PTAA balance gradient (1950–2004) with the four different Bering Glacier System hypsometric curves.

Outline/ Hypsometry	bn (m/yr w.e.)	Volume Change (km^3/yr)	Sea Level Equivalent (mm/yr)	% of Alaska Contribution
AH	−4.4	−10.3	0.0297	21.2
T1H	−3.7	−11.2	0.0324	23.1
BH	−2.0	−7.3	0.0210	15.0
T2H	−1.6	−7.5	0.0217	15.5

EGU

Improving estimation of glacier volume change

M. J. Beedle et al.

Full Screen / Esc

Printer-friendly Version

Interactive Discussion

EGU

Table 4. Debris-cover adjusted PTAA mass balance results. Mass balance, volumetric change, and SLE results from integrating the debris-cover adjusted PTAA balance gradient (1950–2004) with the four different Bering Glacier System hypsometric curves.

Outline/ Hypsometry	bn (m/yr w.e.)	Volume Change (km^3/yr)	Sea Level Equivalent (mm/yr)	% of Alaska Contribution
AH	−3.2	−7.3	0.0211	15.1
T1H	−2.7	−8.2	0.0236	16.9
BH	−1.2	−4.2	0.0122	8.7
T2H	−1.0	−4.6	0.0131	9.4

Improving estimation of glacier volume change

M. J. Beedle et al.

EGU

Table 5. Template method mass balance results. Mass balance, volumetric change, and SLE results from integrating the template method mass balance results with the four different Bering Glacier System hypsometric curves. Template method results also represent a 1950–2004 average as the average ELA of 1500 m (derived from the PTAA model) is used to define benchmark glacier AAR values.

Outline/ Hypsometry	bn (m/yr w.e.)	Volume Change (km^3/yr)	Sea Level Equivalent (mm/yr)	% of Alaska Contribution
AH	−3.0	−7.0	0.0200	14.3
T1H	−2.5	−7.6	0.0220	15.7
BH	−1.2	−4.4	0.0126	9.0
T2H	−1.1	−5.2	0.0151	10.8

**Improving estimation
of glacier volume
change**

M. J. Beedle et al.
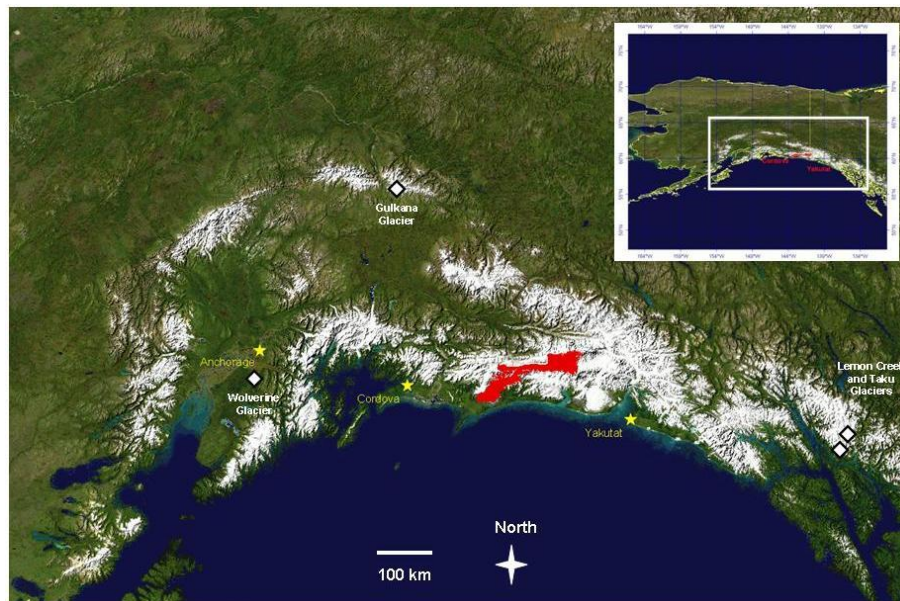
Fig. 1. Location of Bering Glacier System, Alaska. Bering Glacier System is shaded in red. The two meteorological stations used in the PTAA model, Yakutat and Cordova (yellow stars), are indicated to the west and east of Bering Glacier System. The four glaciers with tempo-rally significant mass balance records in southern and southeast Alaska, which were tested as possible benchmark glaciers, are also indicated (white and black diamonds).

EGU

EGU
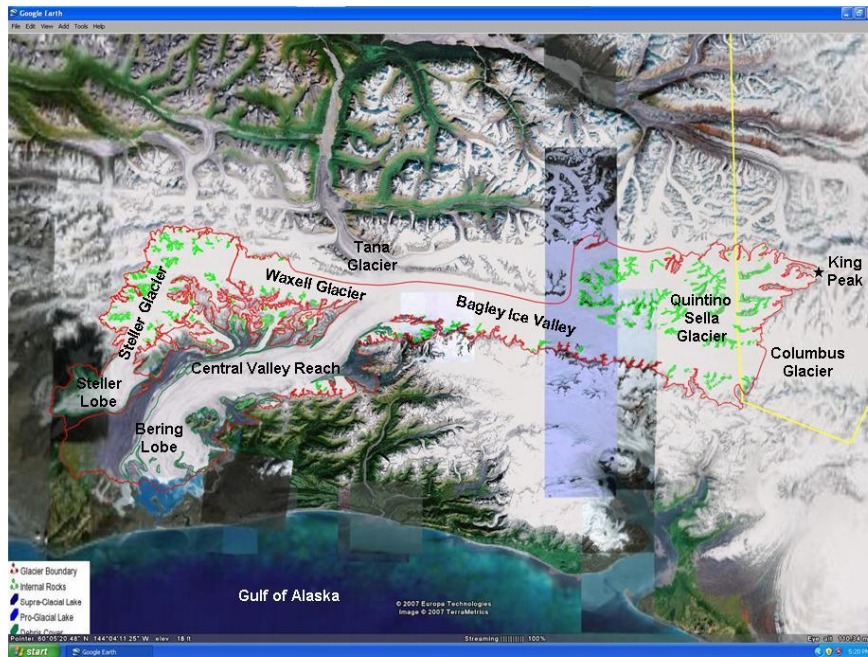
Fig. 2. Bering Glacier System, Alaska. Glacier outlines digitized in GLIMSView displayed in Google Earth™. The Surging Bering Glacier (SBG) and Steller Glacier are outlined in red. Together the SBG and Steller Glacier comprise the complete Bering Glacier System – as is recognized by the U.S. Board on Geographic Names. Nunataks are outlined in light green and debris covered areas are outlined in dark green.
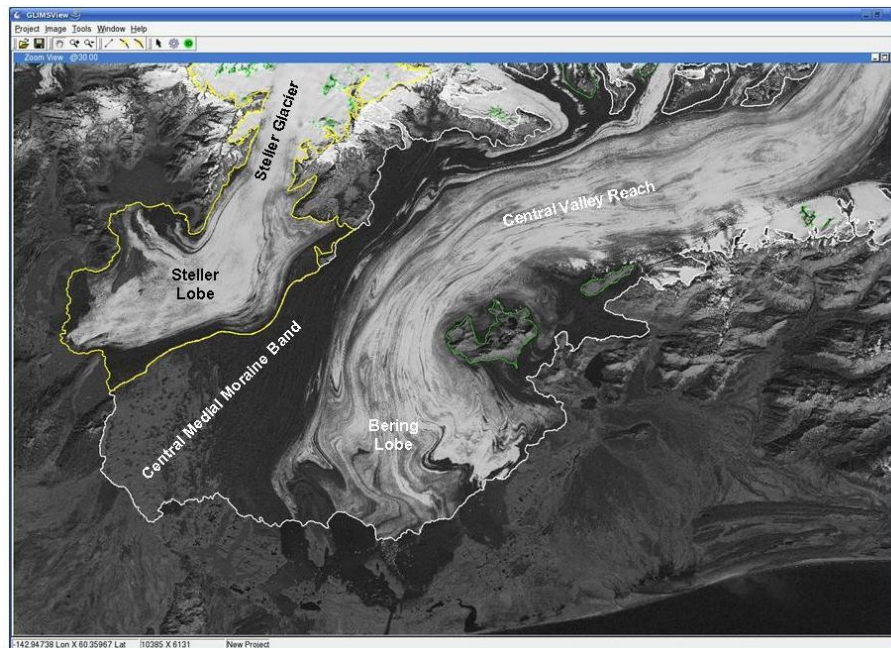
Fig. 3. Bering Glacier piedmont lobe. This GLIMSView screen image displays the Landsat ETM+ panchromatic band (10 September 2001) used to outline the termini of the Bering Glacier System. The Steller Glacier is outlined in yellow and the Surging Bering Glacier System is outlined in white. Nunataks are outlined in green. Bering Glacier officially refers to the large piedmont lobe which includes the Steller Lobe, Central Medial Moraine Band, Bering Lobe and Central Valley Reach.

EGU
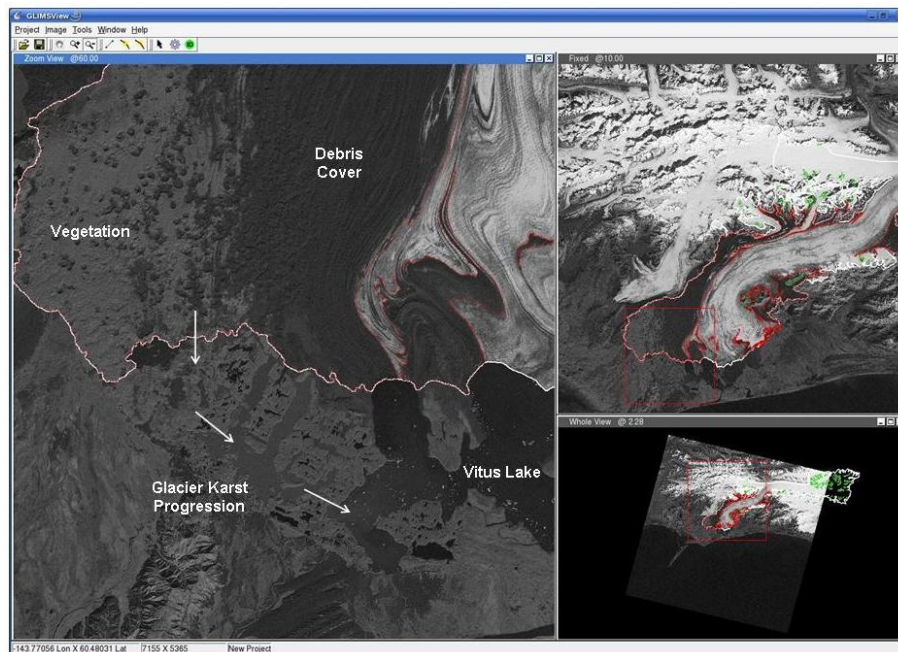
Fig. 4. Surging Bering Glacier System debris cover. This GLIMSView screen image displays the Landsat ETM+ panchromatic band (10 September 2001) used to outline the termini of the Bering Glacier System. The Surging Bering Glacier System is outlined in white and the area defined as debris cover is outlined in red. Nunataks are outlined in green. Note the large glacierized area covered by vegetation, the apparent thickness and continuity of debris cover, and the progressive stages of glacier karst.
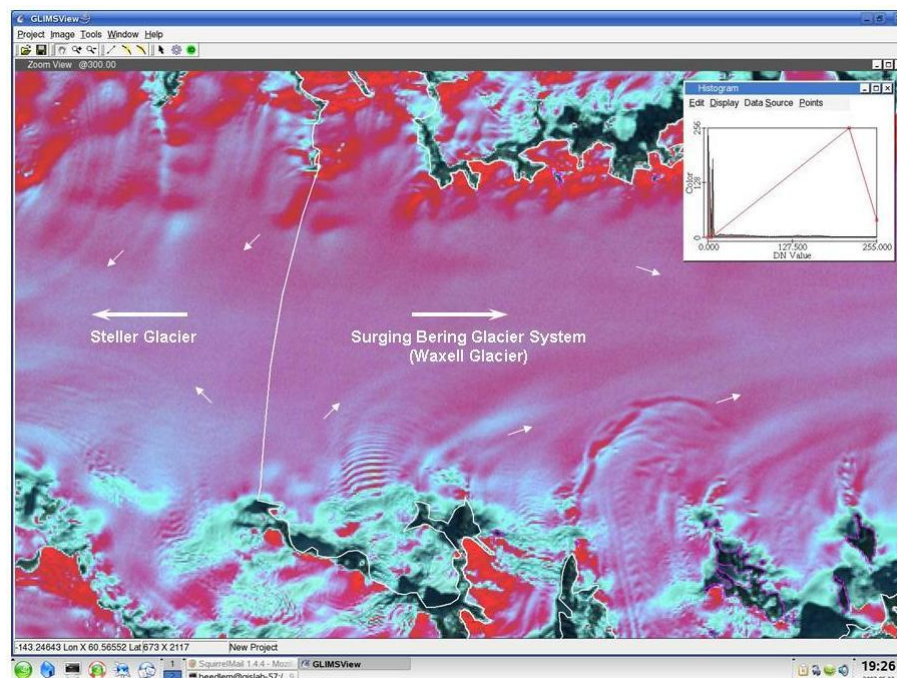
Fig. 5. Steller Glacier and Surging Bering Glacier System flow divide. This GLIMSView screen image shows the flow divide between the Steller Glacier and Surging Bering Glacier System (Waxell Glacier). A composite of Landsat ETM+ bands 4,3, and 2 (31 August 2000) has been "stretched" within the histogram function of GLIMSView (see inset). Such stretching helps to visualize linear surface features (indicated by small white arrows) indicative of glacier flow. The Surging Bering Glacier System outline is in white.

EGU
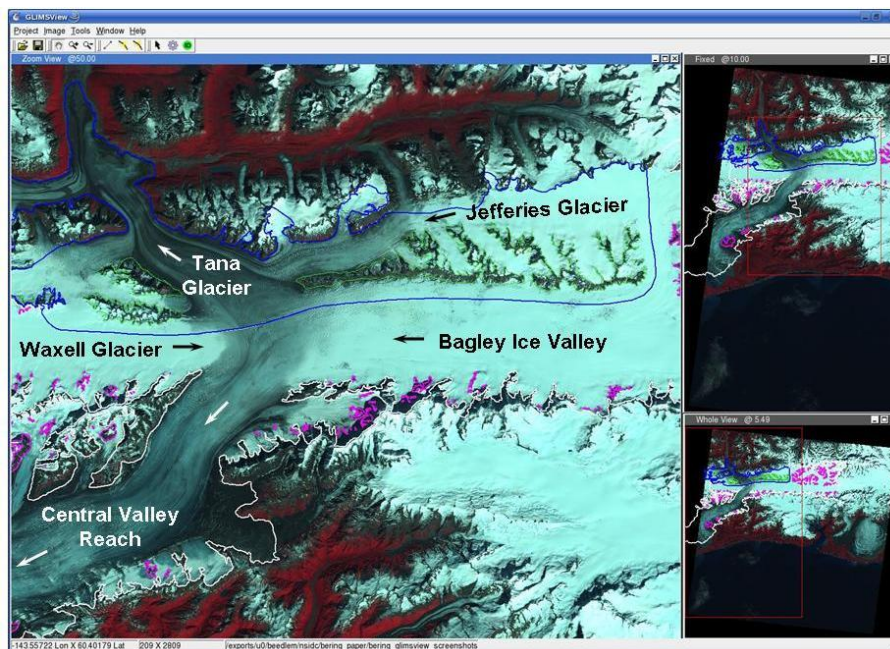
Fig. 6. Tana Glacier and Surging Bering Glacier System divide. This GLIMSView screen image shows the complex flow divide between the Tana Glacier and Surging Bering Glacier System (SBG). This is the same composite of Landsat ETM+ bands 4, 3, and 2 (31 August 2000) shown in Fig. 2, but without band stretching. Tana Glacier is outlined in blue and Tana Glacier nunataks are outlined in green. SBG is outlined in white with nunataks outlined in purple. Note the medial moraines of Tana Glacier and ice between them, which qualitatively indicates the amount of contributing ice and from where it flows.

EGU
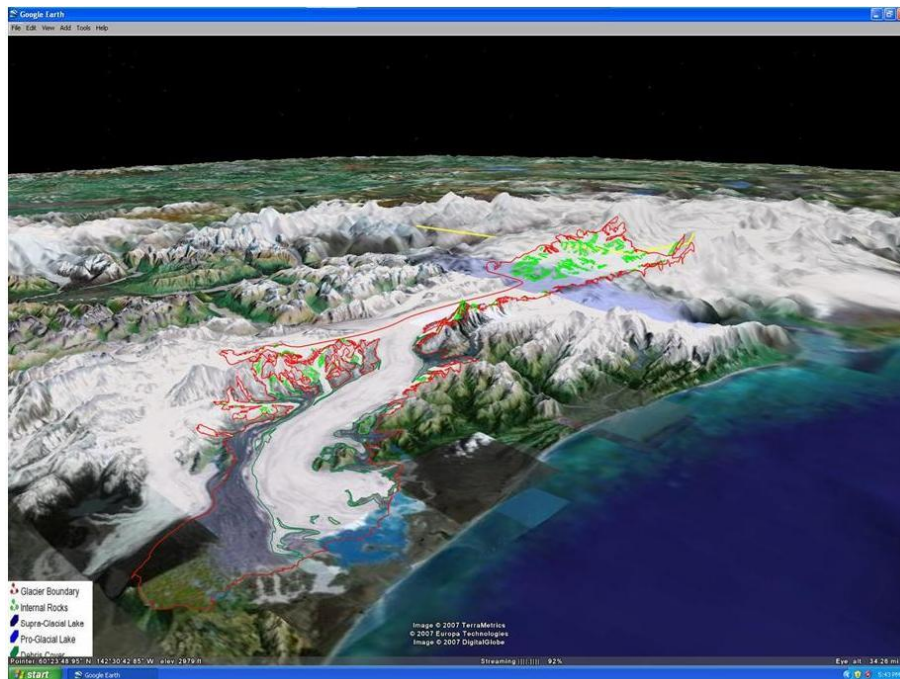
Fig. 7. Surging Bering Glacier System. Looking norththeast on the Surging Bering Glacier System outline digitized in GLIMSView and displayed in Google Earth™ with a 3 fold vertical exaggeration. The glacier outline is in red, nunataks are outlined in light green, and debris cover is outlined in dark green.
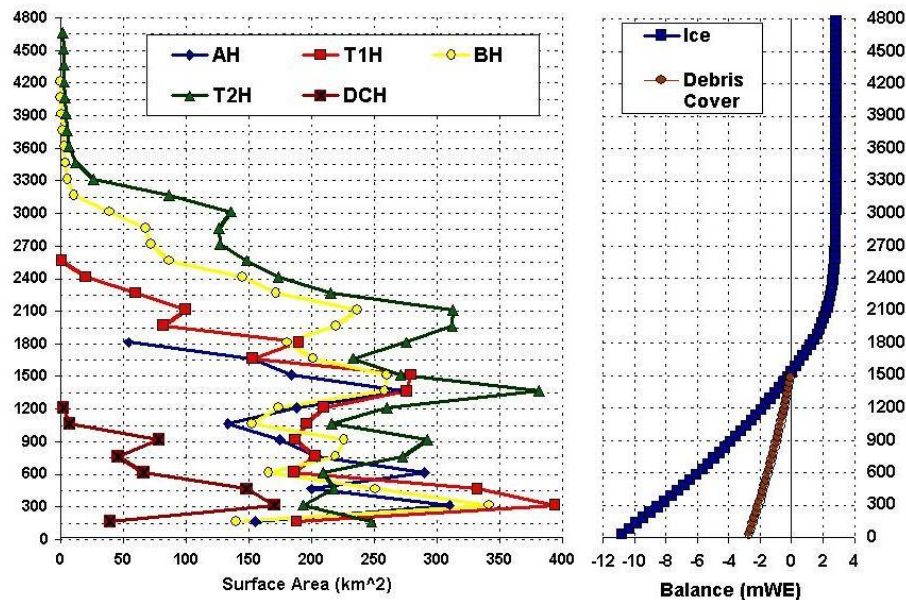
Fig. 8. Area-altitude distributions of four Bering Glacier System outlines and the PTAA mass balance gradients. The graph on the left shows Bering Glacier System surface area within 150 m elevation bands for each of the four outlines and debris cover. The graph on the right is the average (1950–2004) PTAA modeled mass balance gradient.

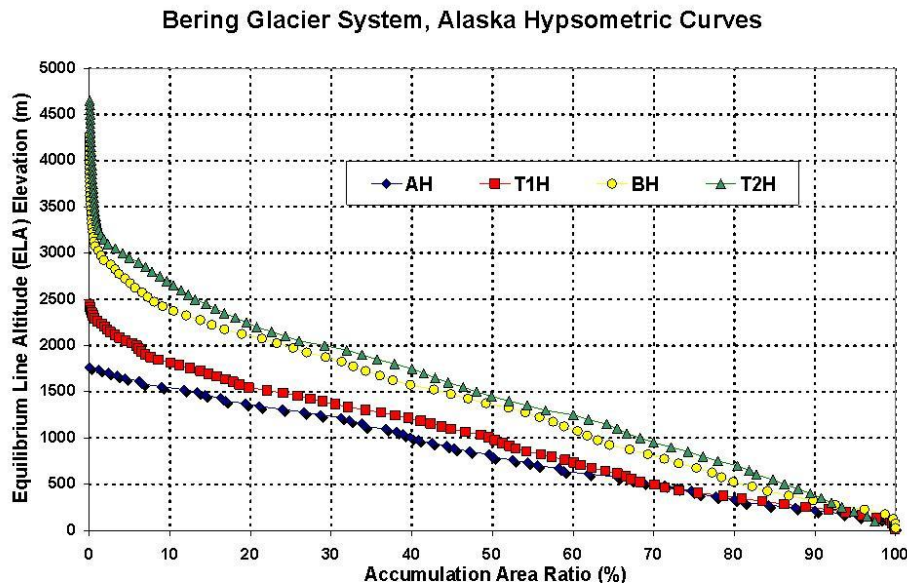**Bering Glacier System, Alaska Hypsometric Curves**

Fig. 9. Hypsometric Curves of Four Bering Glacier System Outlines. Hypsometric curves of the four Bering Glacier System outlines used in this study. Note the gross disparity between AAR values with a common ELA. An ELA of 1500 m yields AAR values of 12, 22, 43, and 46 for the AH, T1H, BH, and T2H outlines respectively. Note also, the linear nature of the hypsometric "curves" – indicating the relatively consistent amount of area within elevation bins, and the generally rectangular shape of Bering Glacier System.

EGU